



Evaluation of the Effect of the Size of *Ramalina fraxinea* Based Ag NPs on the Antimicrobial Activity*

Almustafa Mahdi Saleh ALFAWADI^{1,a}, Mehmet Gökhan HALICI^{2,b}, Fatih Dogan KOCA^{3,c}

¹Erciyes University, Institute of Science, Department of Biology, Kayseri-TÜRKİYE

²Erciyes University, Faculty of Science, Department of Biology, Kayseri- TÜRKİYE

³Erciyes University, Faculty of Veterinary Medicine, Department of Aquatic Animals, Kayseri- TÜRKİYE

ORCID: ^a0000-0001-9365-537X; ^b0000-0003-4797-1157; ^c0000-0001-9774-3019

Corresponding author: Almustafa Mahdi Saleh ALFAWADI; E-mail: mostly.ml@gmail.com

How to cite: Alfawadi AMS, Halıcı MG, Koca FD. Evaluation of the effect of the size of *Ramalina fraxinea* based Ag NPs on the antimicrobial activity. Erciyes Univ Vet Fak Derg 2023; 20 (1): 1-7

Abstract: For the first time in this study, the effect of nanoparticles (NP) sizes on the antimicrobial activity of Ag NPs of different sizes obtained by the reaction of *Ramalina fraxinea* (*R. fraxinea*) extract and silver nitrate (AgNO₃) at different concentrations was evaluated. For this purpose, characteristic light absorption points, and charge of the surface were determined by ultraviolet-visible spectroscopy (UV-Vis), and zeta potential, hydrodynamic diameters by dynamic light scattering (DLS) analysis, morphology, and diameters of NPs were determined by scanning electron microscope (SEM) analysis. The crystal structures of Ag NPs were confirmed by the X-ray diffraction (XRD) analysis map. The functional groups of the *R. fraxinea* extract, which plays an active role in the synthesis of Ag NP, were revealed by the peaks obtained by Fourier transform infrared spectroscopy (FT-IR) analysis. As a result of the characterization tests, the average diameter of Ag NPs increased from 14 nm to 48 nm with the increase in Ag NO₃ concentration used in the synthesis of Ag NP (from 10⁻³ M to 5*10⁻² M). The antimicrobial activity of Ag NPs against *Staphylococcus aureus*, *Escherichia coli*, and *Candida albicans* strains was evaluated depending on the size of the NPs. The antimicrobial effect of small-sized Ag NPs against the studied strains was quite effective compared to large-sized Ag NPs. As a result, it is seen that Ag NPs synthesized by using *R. fraxinea* extract in different sizes with a biologically inexpensive and eco-friendly method exhibit antimicrobial activity depending on the size. It is thought that the study data will be a guide for nanotechnology and biomedical field studies.

Keywords: Antimicrobial activity, biosynthesis, *Ramalina fraxinea*, silver nanoparticles

***Ramalina fraxinea* Bazlı Ag NP'lerin Boyutunun Antimikrobiyal Aktiviteler Üzerindeki Etkisinin Değerlendirilmesi**

Öz: Bu çalışmada ilk kez *Ramalina fraxinea* özütü ile farklı konsantrasyonlarda AgNO₃ reaksiyonu sonucunda elde edilen farklı boyutlara sahip Ag NP'lerin karakterizasyonları değerlendirilmiştir. Bu amaçla NP'lerin UV-Vis. analizi ile karakteristik ışık emme noktaları, zeta testi ile yüzey yükleri DLS analizi ile hidrodinamik çapları, SEM analizi ile NP'lerin morfoloji ve çapları tespit edilmiştir. Ag NP'lerin kristal yapıları XRD haritası ile doğrulanmıştır. Ag NP'nin sentezinde aktif olarak rol oynayan *R. fraxinea* özütünün fonksiyonel grupları FT-IR analizi ile elde edilen pikler ile ortaya konmuştur. Yapılan karakterizasyon testleri sonucunda Ag NP'nin sentezinde kullanılan Ag NO₃ konsantrasyonunun artışı ile birlikte (10⁻³ M-5*10⁻² M) AgNP'lerin ortalama çapı 14 nm'den 48 nm'ye artış göstermiştir. *Staphylococcus aureus*, *Escherichia coli* ve *Candida albicans* suşlarına karşı Ag NP'lerin antimikrobiyal etkinliği NP'lerin boyutuna bağlı olarak değerlendirilmiştir. Küçük boyuta sahip Ag NP'lerin çalışılan suşlara karşı antimikrobiyal etkisi büyük boyuta sahip AgNP'lere göre oldukça etkilidir. Sonuç olarak *R. fraxinea* özütü ile biyolojik olarak ucuz etkili ve çevre dostu yöntemle farklı boyutlarda sentezlenen AgNP'lerin boyuta bağlı olarak antimikrobiyal aktivite sergilediği görülmektedir. Çalışma verilerinin nanoteknoloji ve biyomedikal alan çalışmaları için yol gösterici olacağı düşünülmektedir.

Anahtar kelimeler: Antimikrobiyal aktivite, biyolojik sentez, *Ramalina fraxinea*, gümüş nanopartikülleri

Introduction

Microorganisms have become resistant to antibiotics, which gave scientists and researchers an incentive to search for new methods that contribute to the prevention and drug delivery in a good, different, and inexpensive way. Technology and its development play

an important role, as it contributed to the development of nanotechnology, which has many applications in various fields, including scientific, engineering, medical and industrial applications (Sajid et al., 2015). It has been noted that nanoparticles exhibit superior antimicrobial, anticancer, and catalytic activity due to their small size ranging from 1-100 nm, large surface areas, and high surface energies (Koca et al., 2019). The green methods for the synthesis of nanoparticles are developing into an important

Submission Date/Geliş Tarihi : 15.06.2022
Accepted Date/Kabul Tarihi : 05.10.2022

*This study produced from the thesis of corresponding author

branch of nanotechnology due to the increasing necessity to develop eco-friendly technologies in material synthesis (Basavaraja et al., 2008). For example, the biosynthesis of inorganic compounds particularly metal nanoparticles was acted by using fungus (Vigneshwaran et al., 2006; Vigneshwaran et al., 2007), microorganisms (Shahverdi et al., 2007), plants (Ceylan et al., 2021), DNA (Ocsoy et al., 2013), etc. While microorganisms such as bacteria, actinomycetes, and fungi are still being studied for metal nanoparticle production, using sections of whole plants in comparable nanoparticle synthesis approaches is an exciting and under-exploited potential. Gold NPs are deemed biocompatible, chemical synthesis procedures may result in the existence of poisonous chemical species absorbed on the surface, which could have negative implications in medical applications (Dubey et al., 2010). The use of microorganisms, plants, or lichens to the synthesis of NPs could potentially solve this problem by making the nanoparticles more biocompatible (Sougandhi and Ramanaiah, 2020). The use of plant extract for nanoparticle synthesizing could be more eco-friendly than other biological procedures since it eliminates the time-consuming process of maintaining cell cultures. The synthesis of Au and Ag NPs by using plant extracts was initially described by (Gardea-Torresdey et al., 2002, 2003). The green synthesis of metallic NPs using plant extract or biomass, as shown above, is a promising application. Green Ag NPs have recently been synthesized using natural products such as leaf extract of *Calliandra haematocephala* (Raja et al., 2017), and *Azadirachta indica* leaf extract (Roy et al., 2017).

Lichen is a unique organism because of its biologically active substances, many of these substances have been discovered to have a variety of biological actions in recent years, including anticancer, antibacterial, antifungal, anti-inflammatory, antiproliferative, cytotoxic, and antioxidant properties (Kosanić et al., 2011; Özen et al., 2008). The antibacterial activities and antioxidant qualities of lichen species have been tested versus bacteria in recent studies (Manojlović et al., 2012). In previous studies, the presence of usnic acid in the content of *Ramalina fraxinea* has been revealed (Santiago et al., 2010; Shukla et al., 2010; Sesal et al., 2016). Zinc oxide (ZnO) NPs synthesized by using *Ramalina fraxinea* extract synthesized by Koca et al. 2019, to investigate the cytotoxic effects of NPs on human neuroblastoma cells (Koca et al., 2019). While studies of the antimicrobial activities of metallic NPs synthesized with various bioextracts were found in the literature, it was observed that there are limited studies on the determination of the antimicrobial activities of lichen extract-based Ag NPs with different sizes.

In this study, size depended antimicrobial activities of Ag NPs synthesized with *Ramalina fraxinea* extract

were evaluated depending on their size. For this purpose, different sizes of Ag NPs were synthesized and characterized as a result of the reaction of different concentrations of Ag ions and lichen. Finally, the antimicrobial effects of Ag NPs synthesized in different sizes were shown.

Materials and Methods

Preparation of lichen extract

Ramalina fraxinea samples collected from Kayseri are shown in Figure 1. The samples brought to the laboratory were washed, dried, and preserved for use in NP synthesis. About 10 g dried lichen samples were held in 100 ml distilled water at 80°C for 1 h. Then the solution was filtrated via Whatman No 1 filter paper and stored at +4°C.



Figure 1. *Ramalina fraxinea*.

Synthesis of Ag NPs

For the synthesis of different sizes of Ag NPs extract and different concentrations of AgNO₃ (10⁻² M, 5x10⁻² M, 10⁻³ M, 5x10⁻³ M) were mixed (9:1 ratio) in the dark medium at room temperature until the change of color (Figure 2). After ending the reaction the Ag NPs solution was centrifuged (10 mini 4000 rpm). The precipitates were dried (70°C, 1 night) and used for characterization tests.

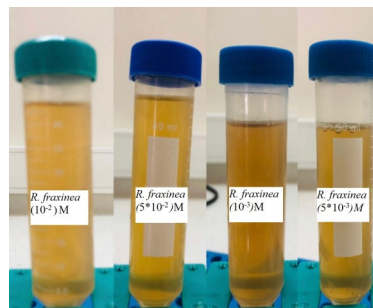


Figure 2. Ag NPs synthesized with *Ramalina fraxinea* different concentrations of AgNO₃.

Determination of antimicrobial activity

Minimum inhibitory concentrations (MICs) of synthesized NPs calculated using the dilution method (96-well plates) to assess antimicrobial susceptibility. The ability of microorganisms (Gram-negative *E. coli*, Gram-positive *S. aureus*, and the fungal pathogen *C. albicans*) to drive observable growth in broth dilutions containing antimicrobial agent dilutions were examined (AgNPs). The MIC is the minimum dose of Ag NP that prevents the tested bacteria from developing for 24 hours at 37°C. The pathogen microorganisms were cultured on Mueller-Hinton broth that was prepared (21/1 g/L) at 15 min. The suspension is adjusted to a turbidity of 0.5 McFarland (MCF), which equates to 1.5x10⁸ bacteria per milliliter.

The following steps were taken to design the 96-well microplate for each microorganism: The antibiotic sensitivity (Ag NPs here) of bacterial strains and fungi were measured using the (A, B, C, D, and E) rows. (F) controlling bacterial activity, (G) microbiological contamination controlling of broth and (H) controlling the microbiological contamination of NPs. The following steps were used to determine the MIC value of each isolated NP, with each extract being investigated in a separate plot. At the first, we add 200 µl of Ag NPs into the well A1. Dispense 100µl of TSB to each of these wells (B1-F1). Then draw 100 µl of Ag NPs from A1 and add it to the well B1 for two-fold serial dilution, draw 100 µl from B1 and add it to the well C1 and mix the content. As before, fill the wells up to E1. Then withdraw from suspension E1 Pipette 100 µl and dispense 100µl bacteria into wells A1 to F1. For controlling the culture, F1 contains a mixture of 200 µl of a bacterial suspension at 0.5 MCF (+control). G1 contains 200 µl of TSB (control). H1 contains 200 µl of NPS (-control). And incubate the 96-wells microplate at 37°C for 24 hours. After 24 hours, pipette 10µL of each row (A1-H1) to be cultured with MHBFigure3.

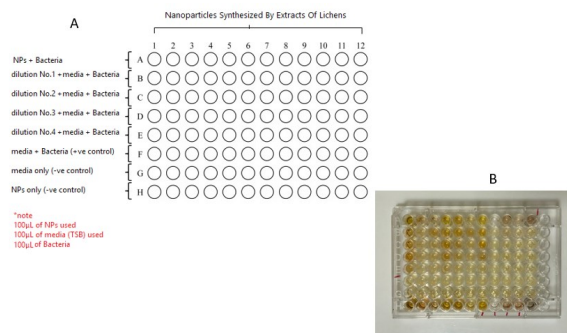


Figure 3. Antimicrobial studies of Ag NPs. A: explaining the design of the microplate; B: 96-wells microplate used in broth microdilution.

Result

UV-vis analysis

The characteristic peak values of *Ramalina fraxinea* extract-based Ag NPs synthesized by using different concentrations of AgNO₃ (10⁻³ M, 5x10⁻³ M, 10⁻² M, and 5x10⁻² M) were determined at 442, 445, 447 and 438 nm, respectively (Figure 4).

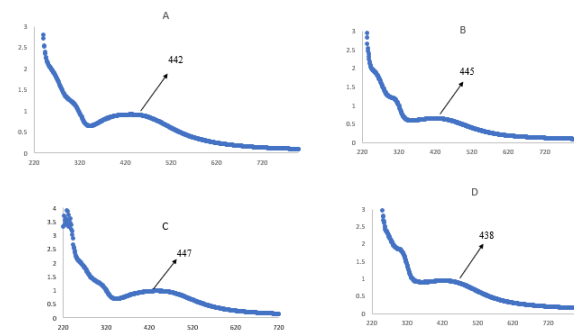


Figure 4. UV analysis of Ag NPs synthesized different concentrations of AgNO₃. A: 10⁻³ M; B: 5x10⁻³ M; C: 10⁻² M; D: 5x10⁻² M.

Zeta potential of Ag nanoparticles

The zeta potential of *Ramalina fraxinea* extracts synthesized different concentration of Ag NO₃ (10⁻³ M, 5X10⁻³ M, 10⁻² M, 5X10⁻² M) were determined at (-8.14 mV, -9.72 mV, -4.54 mV and -3.96 mV) respectively (Figure 5). The negative charge indicated that the Ag NPs were enveloped in the active biological material and were responsible for electrostatic stability.

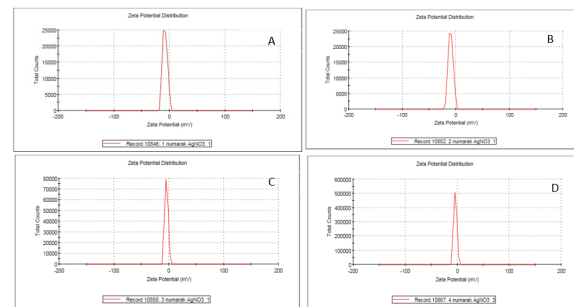


Figure 5. Zeta analysis of Ag NPs synthesized with different concentrations of AgNO₃. A: 10⁻³ M, B: 5x10⁻³ M; C: 10⁻² M; D: 5x10⁻² M.

DLS analysis

DLS analysis has been shown in Figure 6 (a. 10⁻³ M, b. 5x10⁻³ M, c. 10⁻² M, d. 5x10⁻² M). The hydrodynamic diameters of Ag NPs were determined from 360.22 to 447.8 nm (Figure 6).

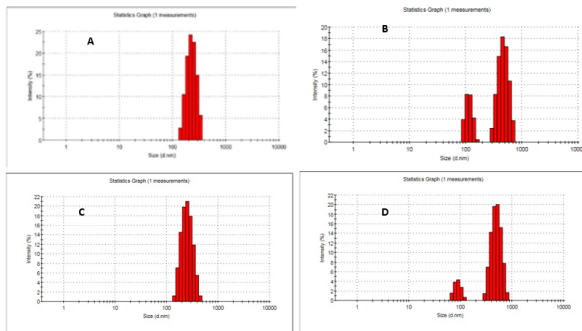


Figure 6. DLS analysis of Ag NPs synthesized with different concentrations of AgNO₃. A: 10⁻³ M; B: 5x10⁻³ M; C: 10⁻² M; D: 5x10⁻² M.

FT-IR analysis

The FT-IR analysis of Ag NPs (Figure 7) synthesized by different concentrations of Ag NO₃ (10⁻³ M, 5x10⁻³ M, 10⁻² M, and 5x10⁻² M) acted for the determined secondary components of *R. fraxiema* extract.

Ag NPs synthesized by using 10⁻³ M AgNO₃ at 3547.4, 2922.4, 2853.4, 1015.4, 972.40, 716.57 and 510.19 cm⁻¹ (Figure 7a), by using 5x10⁻³ M AgNO₃ at 2918.1, 1772.1, 1752.8, 1295.9, 1148.7, 1073.4, 802.57 and 731.62 cm⁻¹ (Figure 7b), by using 10⁻² M AgNO₃ at 1623.8, 1142.2, 1073.4, 1011.1, 933.70, 841.26 and 531.69 cm⁻¹ (Figure 7c), by using 5x10⁻² M AgNO₃ at 2920.83, 1632.23, 1335.87, 1144.01, 1075.39, 840.97, 536.15 and 467.17 cm⁻¹ (Figure 7d).

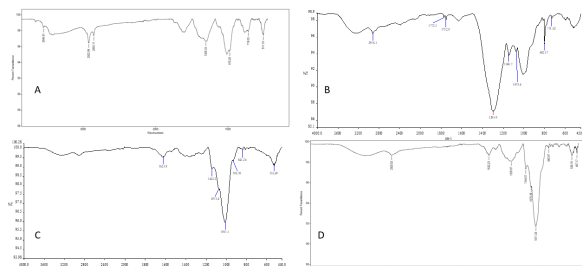


Figure 7. FTIR spectra of Ag NPs synthesized with different concentrations of AgNO₃. A: 10⁻³ M; B: 5x10⁻³ M; C: 10⁻² M; D: 5x10⁻² M.

SEM analysis of Ag NPs

The results of SEM showed particles surround by biomolecules, preventing Ag NPs from aggregating. As shown in Figure 8 the average diameter of Ag NPs synthesized at different concentrations of AgNO₃ (10⁻³ M, 5x10⁻³ M, 10⁻² M, and 5x10⁻² M) were 14 nm, 28.7 nm, 35 nm, and 48 nm respectively.

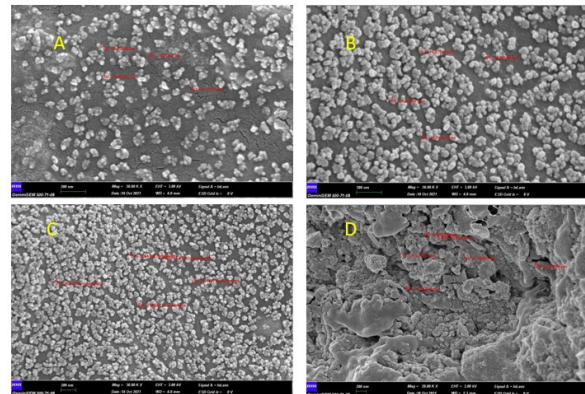


Figure 8. SEM analysis of Ag NPs synthesized with different concentrations of AgNO₃. A: 10⁻³ M; B: 5x10⁻³ M; C: 10⁻² M; D: 5x10⁻² M.

The X-ray diffraction (XRD) analysis of Ag nanoparticles

X-ray diffraction (XRD) pattern of Ag NPs (powder form) was shown Figure 9, and they were taken for the 2θ range (27.8°, 32.6°, 38.1°, 43.12°, 54.4°, 57.4°, 64.7°, and 77.4°). The peaks marked by *Ramalina fraxiema* and the crystal structure of NPs are discussed.

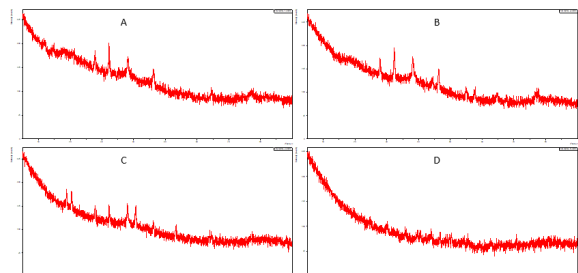


Figure 9. XRD analysis of Ag NPs synthesized with different concentrations of AgNO₃. A: 10⁻³ M; B: 5x10⁻³ M; C: 10⁻² M; D: 5x10⁻² M.

Antimicrobial activity of nanoparticles

In this study, the antibacterial activity of green synthesized Ag NPs were tested against *S. aureus*, *E. coli*, and *C. albicans* at various concentrations, and shown, the minimum inhibitor concentration (MIC) of Ag NPs (14 nm) were determined at 2.1, 8.5, and 2.1 µg/ml, respectively, and results are shown in Table 1 and Figure 10. The MIC values of Ag NPs with 48 nm diameter against all the studied strains were observed at 53.1 µg/ml.

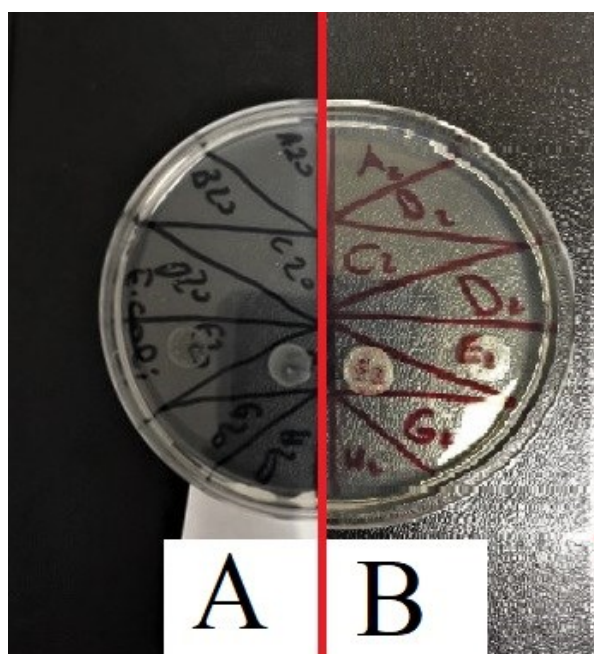


Figure 10. Antimicrobial test results of Ag NPs. (A) *E. coli* growth was observed at dilution 1/16 for (10^{-3} M silver ion); (B) *C. albicans* growth was observed at dilution 1/16 for (10^{-3} M silver ion).

(synthesized with 10^{-3} M, and 5×10^{-3} M AgNO_3), according to the zeta potential value indicating the stability of the NPs. In previous studies, it has been reported that Ag NPs synthesized with different bio-extracts have different zeta charge (Rao et al., 2013; Raja et al., 2017; Erdogan et al., 2019). With the DLS test to determine the effective diameter of dispersed Ag NPs, the effective diameters of the AgNO_3 used in the synthesis increased (from 10^{-3} M to 5×10^{-2} M) with the increase in concentration (from 360 nm to 447 nm). The DLS results of *Calliandra haematocephala*, *Symphytum officinale*, *Coffe arabica*, and *Azadirachta indica* extract-based Ag NPs were determined at 104, 87, 20-30, and 34 nm respectively (Raja et al., 2017; Singh et al., 2018; Dhand et al., 2016; Ahmed et al., 2016). Biofunctional components of *R. fraxinea*, which play a role in the synthesis of Ag NPs, have been identified. According to FT-IR data, C=C (alkene), C-O (aliphatic ether), C-O (primary alcohol), C-O (ether stretch), and C-Cl (halo compound) were determined as *R. fraxinea* biomolecules responsible for the synthesis of Ag NP. The crystal structure of Ag NPs is shown within the XRD diagram. Eight peaks at $2\theta = 27.8^\circ, 32.6^\circ, 38.1^\circ, 43.12^\circ, 54.4^\circ, 57.4^\circ, 64.7^\circ,$ and 77.4° correspond to (1 1 0), (1 2 2), (1 2 3), (2 3 1), (1 4 2), (2 4 1), (2 2 0), (3 1 1) lattice, respectively and suggest that the

Table 1. MIC results of Ag NP ($\mu\text{g/ml}$)

Ag Conc.	Size of Ag NP (nm)	<i>S. aureus</i>	<i>E. coli</i>	<i>C. albicans</i>
10^{-3} M	14	2.1	8.5	2.1
5×10^{-3} M	28.7	10.6	8.5	10.6
5×10^{-2} M	35	42.5	42.5	21.2
10^{-2} M	48	53.1	53.1	53.1

Discussion and Conclusion

The NPs show a surface plasmon resonance (SPR) peak, because of the presence of free electrons, which confirms the formation of Ag NPs. It has been reported that there are shifts in characteristic light absorption points (425-465 nm, 436-448 nm, respectively) depending on the bioagent concentration of Ag NPs synthesized with *Jatropha curcas* and *Azadirachta indica* extracts (Bar et al., 2009, Ahmed et al., 2016). Awwad et al. (2012) reported that the reaction time applied in the synthesis process of Ag NPs is effective in UV bands. In line with these data, the difference in characteristic light absorption points of NPs can be explained by the lichen type, concentration, synthesis conditions, and reaction times that affect the structural properties of NPs. The negative charge indicated that the Ag NPs were enveloped in the active biological material and were responsible for electrostatic stability. Ag NPs synthesized with *R. fraxinea* extract have medium-term stability

silver nanoparticles are crystalline in nature according to planes of a faced center cubic lattice of silver (Mehta et al., 2017). As a result of the reaction of AgNO_3 and *R. fraxinea* extract at increasing concentrations, it was observed that the diameters of Ag NPs increased depending on the concentration increase. While the average diameter of Ag NPs formed as a result of 10^{-3} M AgNO_3 reaction in the environment is 14 nm, the average diameter of Ag NPs formed as a result of 5×10^{-2} M AgNO_3 reaction is 48 nm. In previous studies, it was noted that the diameters of Ag NPs synthesized with *Eriobotrya japonica*, *Salvia spinosa*, and *Berberis vulgaris* extracts ranged from 20 nm (Rao and Ren-Cheng, 2017), to 5 nm (Irtarighat et al., 2019) and 30-70 nm (Behravan et al., 2019), respectively. The functional groups of plants are found in different compositions in different plant species, even in different parts of the same plant. Therefore, the size, shape, and other morphological characteristics of biologically synthe-

sized nanomaterials, can be controlled by the type of plant used. It was determined that Ag NP was synthesized in the shortest time with *Magnolia kobus* extract from the leaf extracts of *Pinus desiflora*, *Ginko biloba*, and *Magnolia kobus* plants. It has been reported that Ag NP was synthesized with *Pinus deciflora* leaf extract at the latest (Song and Kim, 2009). SEM analysis was used to confirm the average diameter of Ag NPs synthesized with different concentrations of AgNO₃ (10⁻³ M, 5*10⁻³ M, 10⁻² M, 5*10⁻² M), the average diameter of Ag NP are 14 nm, 28.7 nm, 35 nm, 48 nm, respectively. (Dubey et al., 2010) reported that the size of Ag NP increases with the increase in the concentration of *Rosa rugosa* extract (from 1 to 5 ml) and Ag ion (from 0.1 to 5 mM).

The nanoparticles have become attached to the wall membrane and also enter inside the bacteria. Ag NPs reaching the cell wall disrupt the structure of the cell wall, produce radical groups, and cause oxidative damage, thus the death of bacteria (Irtarighat et al., 2019). Consistent with our results Behravan et al. (2019) reported that the antimicrobial activities of biologically synthesized Ag NPs were realized by the silver ions released from the NPs and that the NPs with small size exhibited high antimicrobial activity by releasing more Ag ions. The antimicrobial activity of NPs dependson the size and concentration of Ag NPs.

As a result of the characterization tests, it was determined that Ag NPs synthesized as a result of the reaction of *R. fraxinea* extract and AgNO₃ at different concentrations had different morphological and structural properties. In this study, the reduced metal concentration affects many physical parameters, such as the size of the NP, the diameter of the agent, and the zeta charge. In line with the findings obtained, the synthesis of Ag NP was carried out with *R. fraxinea* extract in a cheap, effective and eco-friendly method.

References

- Ahmed S, Saifullah Ahmad M, Swami B L, Ikram S. Green synthesis of silver nanoparticles using *Azadirachta indica* aqueous leaf extract. J Radiat Res App. Sci2016; 9(1): 1-7.
- Awwad AM, Salem NM. Green synthesis of silver nanoparticles by mulberry leaves extract. Nanosci Nanotechno 2012; 2(4): 125-8.
- Bar H, Bhui DK, Sahoo GP, Sarkar P, De SP, Misra A. Green synthesis of silver nanoparticles using latex of *Jatropha curcas*. Colloids Surf A Physicochem Eng 2009; 339(1-3): 134-9.
- Basavaraja S, Balaji SD, Lagashetty A, Rajasab AH, Venkataraman A. Extracellular biosynthesis of silver nanoparticles using the fungus *Fusarium semitectum*. Mater Res Bull 2008; 43: 1164-70.
- Behravan M, Hossein Panahi A, Naghizadeh A, Ziaee M, Mahdavi R, Mirzapour A. Facile green synthesis of silver nanoparticles using *Berberis vulgaris* leaf and root aqueous extract and its antibacterial activity. Int J Biol Macromol 2019; 124: 148-54.
- Ceylan R, Demirbas A, Ocsoy I, Aktümsek A. Green synthesis of silver nanoparticles using aqueous extracts of three *Sideritis* species from Turkey and evaluations bioactivity potentials. Sustain Chem Pharm 2021; 21:100426.
- Dhand V, Soumya L, Bharadwaj S, Chakra S, Bhatt D, Sreedhar B. Green synthesis of silver nanoparticles using *Coffea arabica* seed extract and its antibacterial activity. Mater Sci Eng C2016; 58: 36-43.
- Dubey SP, Lahtinen M, Sillanpää M. Green synthesis and characterizations of silver and gold nanoparticles using leaf extract of *Rosa rugosa*. Colloids Surf A Physicochem Eng 2010; 364(1-3): 34-41.
- Erdogan O, Abbak M, Demirbolat GM, Birtekocak F, Aksel M, Pasa S, Cevik O. Green synthesis of silver nanoparticles via *Cynara scolymus* Leaf Extracts: the characterization, anticancer potential with photodynamic therapy in MCF7 cells. PloS One 2019;14 (6); e0216496.
- Gardea-Torresdey JL, Gomez E, Peralta-Videa J, Parsons JG, Troiani HE, Jose-Yacamán M. Alfalfa sprouts: A natural source for the synthesis of silver nanoparticles. Langmuir 2003; 19: 1357-61.
- Gardea-Torresdey JL, Parsons JG, Dokken K, Peralta-Videa J, Troiani HE, Santiago P, Jose-Yacamán M. Formation and growth of Au nanoparticles inside live alfalfa plants. Nano Lett 2002; 2: 397-401.
- Irtarighat S, Ghannadnia M, Baghshahi S. Green synthesis of silver nanoparticles using the plant extract of *Salvia spinosa* grown in vitro and their antibacterial activity assessment. J. Nanostructure Chem 2019; 9:1-9.
- Koca FD, Ünal G, Halici MG. Lichen based synthesis of zinc oxide nanoparticles and evaluation of its neurotoxic effects on human neuroblastoma cells. J Nano Res 2019; 59: 15-24.
- Kosanić M, Ranković B, Vukojević J. Antioxidant properties of some lichen species. J Food Sci Technol 2011; 48: 584-90.
- Manojlović N, Ranković B, Kosanić M, Vasiljević P, Stanojković T. Chemical composition of three parmelia lichens and antioxidant, antimicrobial and cytotoxic activities of some their major metabolites. Phytomedicine 2012; 19(13): 1166-72.

- Mehta BK, Chhajlani M, Shrivastava BD. Green synthesis of silver nanoparticles and their characterization by XRD. J Phys Conf Ser 2017; 836: 1-4.
- Ocsoy I, Gulbakan B, Chen T, Zhu G, Chen Z, Sari M M, Peng L, Xiong X, Fang X, Tan W. DNA-guided metal-nanoparticle formation on graphene oxide surface. Adv Mater 2013; 25: 2319-25.
- Özen T, Kinalioğlu K. Determination of antioxidant activity of various extracts of *Parmelia saxatilis*. Biologia 2008; 63(2): 211-6.
- Raja S, Ramesh V, Thivaharan V. Green biosynthesis of silver nanoparticles using *Calliandra haematocephala* leaf extract, their antibacterial activity and hydrogen peroxide sensing capability. Arab J Chem 2017; 10(2): 253-61.
- Rao B, Ren-Cheng T. Green synthesis of silver nanoparticles with antibacterial activities using aqueous *Eriobotrya japonica* leaf extract. Adv Nat Sci Nanosci Nanotechnol 2017; 8: 015014.
- Rao YS, Kotakadi VS, Prasad TNVKV, Reddy AV, Gopal DS. Green synthesis and spectral characterization of silver nanoparticles from lakshmi tulasi (*Ocimum sanctum*) leaf extract. Spectrochim Acta A Mol Biomol Spectrosc 2013; 103: 156-9.
- Roy P, Das B, Mohanty A, Mohapatra, S. Green synthesis of silver nanoparticles using *Azadirachta indica* leaf extract and its antimicrobial study. Appl Nanosci 2017; 7: 843-50.
- Sajid M, Ilyas M, Basheer C, Tariq M, Daud M, Baig N, Shehzad F. Impact of nanoparticles on human and environment: Review of toxicity factors, exposures, control strategies, and future prospects. Environ Sci Pollut Res 2015; 22(6): 4122-43.
- Santiago KKA, Borricano JNC, Canal JN, Marcelo DMA, Perez MCP, Dela Cruz TEE. Antibacterial activities of fruticose lichens collected from selected sites in Luzon Island, Philippines. Philipp Sci Lett 2010; 3: 18-29.
- Sesal C, Çobanoğlu G, Karaltı İ, Açıkgöz B. In vitro antimicrobial potentials of four Ramalina lichen species from Turkey. Curr Res Environ Appl 2016; 6 (3): 202-9.
- Shahverdi AR, Minaian S, Shahverdi HR, Fakhimi A, Jamalifar H, Nohi AA. Rapid synthesis of silver nanoparticles using culture supernatants of enterobacteria: A novel biological approach. Process Biochem 2007; 42: 919-23.
- Shukla V, Joshi GP, Rawat MSM. Lichens as a potential natural source of bioactive compounds: A review. Phytochem Rev 2010;9: 303-14.
- Singh H, Du J, Singh P, Yi TH. Role of green silver nanoparticles synthesized from *Symphytum officinale* leaf extract in protection against uvb-induced photoaging. J Nanostructure Chem 2018; 8(3): 359-68.
- Song JY, Kim BS. Rapid biological synthesis of silver nanoparticles using plant leaf extracts. Bioprocess Biosyst Eng 2009; 32: 79-84.
- Sougandhi PR, Ramanaiah S. Green synthesis and spectral characterization of silver nanoparticles from *Psidium guajava* leaf extract. Inorg Nano-Met Chem 2020; 50: 1290-4.
- Vigneshwaran N, Kathe AA, Varadarajan PV, Nachane, RP, Balsubramanya RH. Biomimetics of silver nanoparticles by white rot fungus, *Phaenerochaete chrysosporium*. Colloids Surf B Biointerfaces 2006; 53: 55-9.
- Vigneshwaran N, Ashtaputre NM, Varadarajan PV, Nachane RP, Paralikar KM, Balasubramanya RH. Biological silver nanoparticles using the fungus *Aspergillus flavus*. Mater Lett 2007; 61: 1413-18.